Swarm-Echo MGF lv1b Data Calibration Validation Report

Data Calibration Validation Report	Swarm-E Doc. No.	SwarmE-RPT-002
	Revision	-
	Approval Date	2022-05-23
	UI Contract	2021ICA0179

Prepared by:	Robert Broadfoot Graduate Student	DocuSigned by: Robert Broadfoot 029C82F304254E0...	5/24/2022
Reviewed & Approved by:	Andrew Howarth Swarm-Echo Mission Manager	DocuSigned by: 85257CF9BD56409...	5/23/2022
Reviewed & Approved by:	David Miles Swarm-Echo MGF Instrument PI	DocuSigned by: E894F56008E5442...	5/23/2022
Released by:	Katherine Deasy Document Control	DocuSigned by: Katherine Deasy F389A06920E14B9...	5/24/2022

IOWA
Department of Physics and Astronomy

Van Allen Hall
Iowa City, Iowa 52242
Tel: (319) 335-2577
Fax: (319) 335-1753

esa

Revision- released 2022-05-24

Swarm-Echo MGF lv1b Data Calibration Validation Report

Document Revision History			
Revision	**Release Date**	**Description/Changes**	**Change Action #**
RC1	2022-03-14	Release Candidate 1	n/a
-	TBD with watermark	Initial Release. Update to document title per feedback from Antonio de la Fuente. Added applicable and reference documents. Update to orthogonality values due to math error in decomposition math.	n/a

To Be Confirmed (TBC), To Be Determined (TBD), and To Be Reviewed (TBR)		
Section	**Item**	**Description of Item**

Table of Contents

Table of Exhibits

1 SCOPE

This document serves as an explanation and validation of the results of the in-situ calibration of the MGF sensors on Swarm-Echo. An explanation of the procedure used to calibrate Swarm-Echo can be found in the Swarm-Echo MGF lv1b Data Product Description (SwarmE-RPT-001). Calibration for the MGF sensors was performed in seven-day increments from January 3, 2014, to January 30, 2021. These were performed as new calibrations without the pre-flight calibrations being used as a baseline and are compared to the pre-flight calibration results in Table 1.

2 APPLICABLE AND REFERENCE DOCUMENTS

[AD-1] SwarmE-RPT-001 Swarm-Echo MGF lv1b Data Product Description

[RD-1] Finlay, C. C., Kloss, C., Olsen, N., Hammer, M. D., Tøffner-Clausen, L., Grayver, A., and Kuvshinov, A.: The CHAOS-7 geomagnetic field model and observed changes in the South Atlantic Anomaly, Earth Planets Space, 72, 156, https://doi.org/10.1186/s40623-020-01252-9, 2020.

[RD-2] Matzka, J., Stolle, C., Yamazaki, Y., Bronkalla, O. and Morschhauser, A.: The geomagnetic Kp index and derived indices of geomagnetic activity. Space Weather, https://doi.org/10.1029/2020SW002641, 2021.

[RD-3] Broadfoot, R. M., Miles, D. M., Holley, W., Howarth, A. D.: In-Situ Calibration of the Swarm-Echo Magnetometers, https://doi.org/10.5194/egusphere-2022-59, 2022.

3 CALIBRATION RESULTS

Exhibit 1: Table of Mission Averaged Values

	In-situ Calibration		**Preflight Calibration**	
	Inboard	**Outboard**	**Inboard**	**Outboard**
Sx [eu/nT]	1.0044	1.0024	1.0044	1.0025
Sy [eu/nT]	0.9979	1.0020	0.9984	1.0029
Sz [eu/nT]	1.0503	1.0534	1.0473	1.0519
Oxy [°]	89.87	90.11	90.12	89.93
Oxz [°]	89.71	89.88	90.10	90.02
Oyz [°]	90.01	90.04	89.81	89.93
e1 [°]	2.73	2.68		
e2 [°]	-0.09	0.21		
e3 [°]	2.23	1.96		
offX [nT]	1.47	-199.41		
offY [nT]	2.10	1.20		
offZ [nT]	8.33	24.22		

Mission averaged values for the inboard and outboard sensors compared to the values obtained from the preflight calibrations. The large offset for Outboard X is likely due to a large stray field being generated from the boom near the sensor. Orthogonalities are given in degrees and displayed as 90+Orthogonality.

Magnetometer readings were reduced to 1-Hz from 160-Hz. For calibration, we select data that fall within ± 55° latitude during geomagnetically quiet times. We consider geomagnetically quiet to be when the Kp index (Matzaka et al. 2021) does not exceed 3 or the Dst index does not exceed a change of 3 nT per hour when the data were taken. From the attitude files we flag any data where the attitude solution was not generated by at least one of the star tracker cameras. We also flag any data where the signal has dropped out for greater than ten seconds or there is greater than ten seconds until the next signal is obtained due to potentially large errors when interpolating the attitude solution. Lastly, we flag any data where the rotation rate of the spacecraft exceeds 0.03 degrees/sec.

Accounting for gaps in data coverage or days without usable calibration data, this resulted in 322 individual calibration matrices for each sensor. The individual calibration parameters (sensitivity, orthogonality, Euler angles, and offsets) were decomposed from the calibration matrix and averaged for the entire mission (Exhibit 1). The orthogonality results were then compared to the mission average, and any result that deviated greater than or equal to ± 0.1° was determined to be non-physical, and the entire result for both sensors was replaced with the static mission average. Out of the 322 calibration parameters, 22 (6.8%) were deemed non-physical and replaced with the mission average. Every rejected result occurred prior to the first reaction wheel failure (August 2016) when data coverage in non-polar latitudes was still sparse.

The calibrations were then applied to all the 1-Hz data and compared to the Chaos-7.7 magnetic field model (Finlay et al., 2020). Average residuals and average RMS deviation were calculated for non-polar (+/- 55°) latitudes, for each year in the calibration set (Exhibit 2). Early residuals and RMS errors were higher due to a combination of limited data in the calibration sets and the reaction wheel tone contaminating the sensor readings. Future data releases will focus on increasing the data binned for these calibrations and removing the reaction wheel tone from the sensor data. Even on days with average residuals higher than 1 nT, we are confident with the results of the calibration and with the accuracy of the resulting sensor data. This document will be updated for future data releases.

Exhibit 2: Average Residuals, Average RMS Error

	Inboard													
	2014		**2015**		**2016**		**2017**		**2018**		**2019**		**2020**	
	mean	**rms**	**mean**	**rms**	**mean**	**rms**	**mean**	**rms**	**mean**	**rms**	**mean**	**rms**	**mean**	**rms**
B_x	-2.80	13.97	-2.91	14.61	-0.21	13.73	0.61	13.23	0.40	12.79	0.33	11.65	0.26	11.58
B_y	0.86	20.34	-0.81	22.13	0.15	11.19	-0.04	10.64	0.16	10.30	0.27	9.91	-0.14	9.32
B_z	-1.53	10.71	0.75	12.12	-0.18	11.26	0.09	10.77	-0.17	10.84	0.03	11.11	0.00	10.67
$\|B\|$	-2.80	16.21	-2.91	19.23	-0.21	9.23	0.61	9.76	0.40	9.05	0.33	8.81	0.26	8.85
	Outboard													
	2014		**2015**		**2016**		**2017**		**2018**		**2019**		**2020**	
	mean	**rms**	**mean**	**rms**	**mean**	**rms**	**mean**	**rms**	**mean**	**rms**	**mean**	**rms**	**mean**	**rms**
B_x	2.87	17.12	3.63	18.73	0.46	13.58	0.53	12.99	0.42	12.67	0.27	11.71	0.07	11.61
B_y	1.27	14.70	-1.29	14.92	0.17	11.22	-0.10	10.48	0.28	10.14	0.25	9.80	-0.10	9.17
B_z	-0.52	19.91	1.59	21.99	-0.39	11.00	0.13	10.40	-0.23	10.41	0.02	10.64	-0.01	10.15
$\|B\|$	2.87	11.35	3.63	13.28	0.46	8.81	0.58	9.34	0.42	8.57	0.27	8.45	0.07	8.33

Average residuals and average RMS error for non-polar latitudes by year. The largest change in average residuals occurred between 2015 and 2017, coinciding with the loss of the first reaction wheel and subsequent slowing of the remaining wheel rates. The steady improvement in the results every year after can be attributed to the increased data coverage.

To further validate the calibration results we calculated the residuals for all 1-Hz data compared to the Chaos model for the calibration set until the start of 2021 (Exhibit 3). The results show, as expected, that the residuals in the non-polar latitudes (+/- 55°) are small and increase in the auroral latitudes. The darker area in the residuals represents the rms error for the residuals at that degree of latitude.

Exhibit 3: Calibrated 1-Hz Residuals

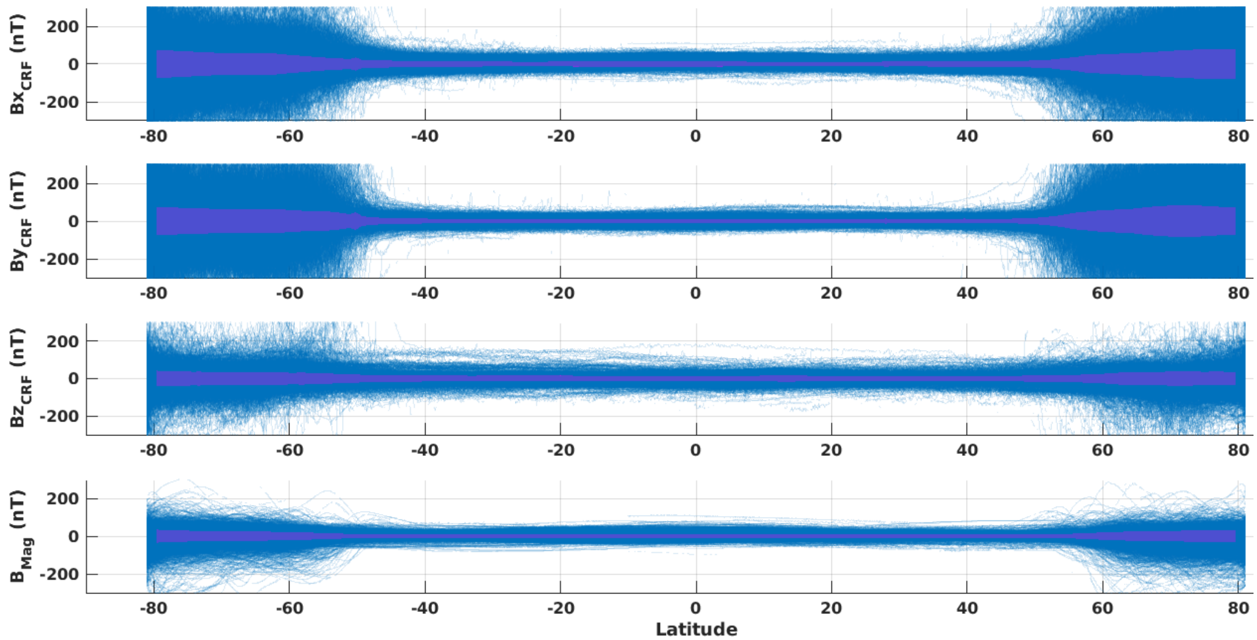

All calibrated 1-Hz residuals for the outboard sensor with the Chaos model versus latitude. The same data culling as in section 6 was used for this plot and any data that did not meet that criterion was not included. The darker section in the data represents the RMS error for the data binned by each degree of latitude.